THE JOURNAL OF BIOLOGICAL CHEMISTRY Vol. 278, No. 42, Issue of October 17, pp. 41420–41430, 2003

Printed in U.S.A.

The Receptor Tyrosine Kinase Regulator Sprouty1 Is a Target of the Tumor Suppressor WT1 and Important for Kidney Development*

Received for publication, June 17, 2003, and in revised form, July 23, 2003
Published, JBC Papers in Press, July 25, 2003, DOI 10.1074/jbc.M306425200

Isabelle Gross‡§¶, Debra J. Morrison‡¶, Deborah P. Hyink‡, Kylie Georgas‖, Milton A. English‡, Mathias Mericskay, Seiyu Hosono‡, David Sassoon**, Patricia D. Wilson‡, Melissa Little‖‡‡, and Jonathan D. Licht‡§§**

*From the ‡Department of Medicine, Mount Sinai School of Medicine, New York, New York 10029, ‖Institute for Molecular Bioscience, University of Queensland, St. Lucia, 4072 Australia, and **Department of Molecular, Cellular and Developmental Biology, Mount Sinai School of Medicine, New York, New York 10029*

***WT1* encodes a transcription factor involved in kidney development and tumorigenesis. Using representational difference analysis, we identified a new set of WT1 targets, including a homologue of the *Drosophila* receptor tyrosine kinase regulator, *sprouty*. *Sprouty1* was up-regulated in cell lines expressing wild-type but not mutant WT1. WT1 bound to the endogenous *sprouty1* promoter *in vivo* and directly regulated *sprouty1* through an early growth response gene-1 binding site. Expression of Sprouty1 and WT1 overlapped in the developing metanephric mesenchyme, and Sprouty1, like WT1, plays a key role in the early steps of glomerulus formation. Disruption of Sprouty1 expression in embryonic kidney explants by antisense oligonucleotides reduced condensation of the metanephric mesenchyme, leading to a decreased number of glomeruli. In addition, *sprouty1* was expressed in the ureteric tree and antisense-treated ureteric trees had cystic lumens. Therefore, *sprouty1* represents a physiologically relevant target gene of WT1 during kidney development.**

The development of the mammalian metanephric kidney is a model for the study of cellular and molecular mechanisms of organogenesis (1). Wilms tumor, a pediatric kidney malignancy, is characterized by a triphasic histopathology (blastemal, stromal, epithelial) signifying an abnormal differentiation program. In accordance with this notion, the Wilms Tumor suppressor gene 1 (*WT1*), inactivated in a subset of Wilms tumors, plays an essential role in normal development of the kidney and the genitourinary system (2–4). Targeted disruption of *WT1* in mice leads to a complete agenesis of the kidneys and gonads (5). The specific temporal and spatial pattern of *WT1* expression suggests multiple roles for WT1 during nephrogenesis. In particular, *WT1* expression peaks during the mesenchymal-to-epithelial transition (MET),[1] suggesting an instructive role in the formation of the renal glomerulus. In the mature kidney, *WT1* expression becomes restricted to the podocytes, perhaps being involved in maintaining a differentiated phenotype.

The *WT1* gene encodes a C_2-H_2 zinc finger transcription factor that binds to both GC-rich and TC repeat elements. Alternative splicing at two sites yields four major isoforms, each containing or lacking 17 amino acids between the transactivation domain and the zinc finger region and/or a 3-amino acid insertion (KTS) between the third and fourth zinc fingers. The KTS insertion disrupts the spacing between the zinc fingers, altering DNA binding (2, 4). The A isoform lacks both these motifs and binds strongly to DNA. The C isoform contains the KTS insertion, displays a weaker DNA binding to alternative sequences, associates with splicing factors, and therefore, may be involved in RNA processing. WT1 binding sites were identified in multiple promoters that respond to WT1 in transient transfection assays (2, 6, 7); however, most are not regulated by WT1 *in vivo* (8). Thus, identification of *bona fide* target genes would provide insight into WT1 function in development and tumorigenesis.

We previously showed that NIH3T3 cells engineered to express the WT1A isoform were growth-inhibited and displayed partial epithelial differentiation (9). These morphological changes correlated with significant alterations in gene expression consistent with a role for WT1 in the MET. Here, we applied cDNA representational difference analysis (RDA (10)) to NIH3T3 cells *versus* WT1-expressing NIH3T3 cells and identified *sprouty1* (*spry1*), a mammalian homologue of *Drosophila sprouty*, as a gene up-regulated in response to WT1. *Drosophila sprouty* was first identified as an antagonist of the branching morphogenesis of the tracheal system and was genetically shown to inhibit receptor tyrosine kinase signaling (11, 12). To date, four vertebrate *spry* genes have been identified (13–17). The proteins they encode share a conserved, cysteine-rich C-terminal domain and a more divergent N-terminal domain. On a molecular level, these proteins were shown to down-regulate signaling by many receptor tyrosine kinases, with the notable exception of the epidermal growth factor receptor, where *sprouty* appears to increase the action of the protein (18–23). In NIH3T3 cells Spry1 and Spry2 antagonized signaling through multiple receptor tyrosine kinases by specific inhibition of the

* This work was supported by National Institutes of Health Grant CA59998, the T. J. Martell Foundation for Cancer, AIDS, and Leukemia Research (to J. D. L.), the Association Pour La Recherche sur le Cancer (to I. G.), the American Foundation for Urologic Disease (to D. M.), and the National Health and Medical Research Council, Australia (to M. L.). Confocal microscopy performed at the Mount Sinai School of Medicine Microscopy Shared Resource Facility was supported by National Institutes of Health Grant CA95823. The costs of publication of this article were defrayed in part by the payment of page charges. This article must therefore be hereby marked "*advertisement*" in accordance with 18 U.S.C. Section 1734 solely to indicate this fact.

§ Present address: INSERM U381, Strasbourg, France.
¶ These authors contributed equally to this work.
‡‡ A Sylvia and Charles Viertel Senior Research Fellow.
§§ To whom correspondence should be addressed: Box 1130, Mount Sinai School of Medicine, One Gustave L. Levy Place, New York, NY 10029. Tel.: 212-659-5487; Fax: 212-849-2523; E-mail: jonathan.licht@mssm.edu.

[1] The abbreviations used are: MET, mesenchymal-to-epithelial transition; RDA, representational difference analysis; nt, nucleotides; m-, murine; kb, kilobase(s); RT, reverse transcriptase; ISH, *in situ* hybridization; EGR1, early growth response gene-1.

Ras/mitogen-activated protein kinase pathway but not the phosphatidylinositol 3-kinase pathway (23); in this system signal blockade occurred at the level of Ras activation, whereas others reported that Sprouty blocks the activation of Raf (20, 24). Precise spatial and temporal control of the Ras/Raf/mitogen-activated protein kinase cascade, a major pathway for growth factors to mediate cell proliferation or differentiation, is required for normal development. Accordingly, the Spry proteins, which regulate this pathway, were implicated in branching morphogenesis of the lung, angiogenesis, and limb bud outgrowth (14, 25, 26).

In this study, we demonstrated transcriptional regulation of *spry1* by a organ-specific transcription factor, WT1. *spry1* expression was up-regulated by WT1 in several cell lines, and WT1 directly bound and activated the *spry1* promoter. In addition *spry1* was dynamically expressed in the embryonic kidney in a pattern partially overlapping with *wt1*. Disruption of *spry1* expression in kidney explants altered normal glomeruli formation and ureteric tree morphology. Taken together, these results demonstrate that *spry1* is a WT1 target gene that may mediate some of the regulatory effects of WT1 during kidney organogenesis.

MATERIALS AND METHODS

Cell Culture, Transfection, and Infection—NIH3T3, maintained in Dulbecco's modified Eagle's medium with 10% calf serum, were transiently transfected by LipofectAMINE Plus (Invitrogen) using 0.1 μg of the various mouse *spry1* luciferase reporters, 0.005 μg of a thymidine kinase Renilla reporter as internal control, and 1 μg of an empty vector (Rous sarcoma virus) or WT1 expression vectors (Rous sarcoma virus-WT1A and WT1C (27)). Cells were harvested 48 h later and assayed for luciferase activity using a Dual reporter assay (Promega) and for protein expression by immunoblotting. Tet-Off Saos-2 osteosarcoma cells (a gift of Dr. D. Haber, Massachusetts General Hospital) were transfected with a pTRE vector (Clontech) expressing wild-type WT1A, WT1A112, or WT1A129 followed by selection in 0.2 μg/ml puromycin. Retroviral infection (28) and the WT1A-expressing NIH3T3 (9) were described. mIMCD-3 (29) were maintained in Dulbecco's modified Eagle's medium/Ham's F-12 medium with 10% fetal calf serum.

RDA—Double-stranded cDNAs were synthesized with 5 μg of poly(A)$^+$ RNA from NIH3T3 and WR16 cells, and RDA was performed (10). To identify genes activated by WT1, three rounds of RDA subtracting the 3T3 representation from the WR16 representation were performed (WR16–3T3). To identify repressed genes, the reciprocal subtractions were done in parallel (3T3-WR16). The differential products were subcloned into pBluescript SK− (Stratagene). To confirm that the cDNA fragments were present in different amounts, each was ^{32}P-labeled and used as a probe to hybridize blots of NIH3T3 or WR16 representations. This step eliminated false positives (30%) before sequencing.

Cloning of the spry1 cDNA—The nucleotide (nt) positions for murine *spry1* (m*spry1*) are listed under AF176903. From RDA, a cDNA corresponding to nt 1079–1693 of m*spry1* was isolated and used to identify an EST (GenBank™ AA591484, clone ID 907842) containing nt 962–2489 of m*spry1*. The 5′ end of m*spry1* was obtained by rapid amplification of cDNA ends PCR (Marathon cDNA amplification kit, Clontech). Briefly, 1 μg of poly(A)$^+$ RNA from podocytes was reverse-transcribed using a m*spry1* primer (nt 1016–1040). After 2nd strand synthesis and ligation to the anchor oligonucleotide, PCR was performed using a primer corresponding to the anchor and a m*spry1* primer (nt 988–1007). The resulting products were subcloned and sequenced. One rapid amplification of cDNA ends product (nt 402–1007 of *mspry1*) was ligated to the above EST clone at a common *Stu*I site. The m*spry*1 coding sequence (nt 481–1469) was amplified by PCR from the full-length cDNA and cloned in-frame with the sequence of the FLAG tag in a modified pcDNA 3–1 (+) vector (30).

spry1 Genomic Cloning and Reporter Plasmids—A bacterial artificial chromosome library was screened (Incyte Genomics, St. Louis, MO) using primers from the m*spry1* cDNA (nt 1171–1191 and 1405–1422) and confirmed by Southern blot with a probe derived from the 5′ end of the m*spry1* cDNA. A 9-kb *Eco*RI fragment encompassing the m*spry1*-coding exon and 5′ and 3′ sequences was subcloned into pBluescript SK+ and sequenced (MWG Biotech Inc). The start site of transcription was mapped by primer extension. A 1.1-kb *Sac*I fragment containing the proximal promoter was ligated into pGL2basic (Promega). A series of 5′ truncations were created by PCR using forward primers located at −614 (5′-GGTACCGGAAGAACCTTGGGC-3′), −354 (5′-GGTACCGGTGGTTTGTTATTG-3′), and −137 (5′-GGTACCTGCTCCGGGTTTTTG-3′) and reverse primer located at +20 (5′-AGATCTGAGCTCTGGCTGCGG-3′) and sub-cloned with *Kpn*I/*Bgl*II into pGL2basic. Mutations of MIN1 (CC**GGGGG**CG to CC**TTTTT**CG-87), MIN2A (GC**GTG**GAGGTG**G** to GC**TTT**GAGGTG**TA**GG**TA**), and MIN2B (GC**GC-GA**CG to GC**TTTT**ACG) binding sites within the SPRY137-luc reporter were created by site-directed mutagenesis (QuikChange, Stratagene).

Electrophoretic Mobility Shift Assay—Double-stranded oligonucleotide probes encompassing eight putative WT1 binding sites within the m*spry1* promoter were end-labeled with [α-^{32}P]dCTP and Klenow. The oligonucleotide probes were: Min1, 5′-GACACATGATATCACCGGGGGCGGGTCCCG-3′; MutMin1, 5′-GACACATGATATCACCTTTTTCGGGTCCCG-3′; Min2, 5′-GTCCCGGCGTGGAGGTGGAGGTGGCGGCGACGCT-3′; Min3, 5′-GCTGCGGAGCCCGCGCGCGAGTGCTCAGCACGCA-3′; Min4, 5′-GCAGGGGTTTGCGGCGGCCCCGCAGCCAGAGCTC-3′; Min5, 5′-TCATTTAAAATGCATTGGTGTTTTGGACAAAA-3′; Min6, 5′-CATTTTTTTTTTCCGTTGTTGGTGGTGGTTTGTTAT-3′; Min7, 5′-CCCTGGAACGCCCGCCCCTCCCCAGTTGCGCTCGCAGG-3′.

In vitro coupled transcription/translations (Promega) were performed with pSP64-WT1A, pSP64-WT1C, and pSP64 control vector. 8 μl of lysate were preincubated for 15 min at room temperature along with 1 μg of poly(dI-dC), 5 μg of bovine serum albumin, and binding buffer (20 mM HEPES, pH 7.5, 70 mM KCl, 5 mM $MgCl_2$, 0.1% Nonidet P-40, 12% glycerol, 0.5 mM dithiothreitol, 100 μM $ZnCl_2$) in a volume of 20 μl followed by the addition of radiolabeled probe (50,000 cpm) for another 15 min. Protein-DNA complexes were resolved on a 5% nondenaturing polyacrylamide gel in 0.5× Tris-buffered EDTA at 300 V for 1.5 h. For competition experiments, 0.4 μg of WT1 antibody (C-19, Santa Cruz) or rabbit IgG (Zymed Laboratories Inc.) or a 1000× excess of cold MIN1, MutMin1, or mut NF-κB (GGCATAGGTCC) oligonucleotides were added during preincubation.

Chromatin Immunoprecipitation—Proteins were cross-linked to DNA by adding formaldehyde directly to the cell media to a concentration of 1% for 10 min at 37 °C. Cross-linking was stopped by the addition of glycine to 0.125 M for 5 min at room temperature. Cells were washed in phosphate-buffered saline and lysed in 1% Nonidet P-40 buffer (150 mM NaCl, 50 mM Tris, pH8, 1% Nonidet P-40, 5 mM EDTA, protease inhibitors) for 30 min at 4 °C. The lysate was sonicated and centrifuged, and the supernatant was diluted 10-fold in 0.1% Nonidet P-40 buffer and precleared with protein G-Sepharose in the presence of 20 μg of salmon sperm DNA and 1 mg/ml bovine serum albumin for 30 min at 4 °C. The supernatant was collected by centrifugation, 1% was saved for total input control, and the remainder was incubated overnight at 4 °C with or without 2 μg of WT1 antibody (F6, Santa Cruz). Immune complexes were collected with protein G-Sepharose for 1 h at 4 °C and washed in the following buffers: A (0.1% SDS, 1% Triton X-100, 2 mM EDTA, 20 mM Tris, pH 8, 150 mM NaCl); B (0.1% SDS, 1% Triton X-100, 2 mM EDTA, 20 mM Tris, pH 8, 500 mM NaCl); C (0.2 M LiCl, 1% Nonidet P-40, 1% sodium deoxycholate, 1 mM EDTA, 10 mM Tris-HCl, pH 8) and twice with Tris-EDTA, pH 8. Immune complexes were eluted with 1% SDS, 0.1 M $NaHCO_3$ followed by gentle centrifugation. Cross-linking was reversed with NaCl (0.2 M) at 65 °C for 4 h, and DNA was recovered by phenol/chloroform extraction and ethanol precipitation. PCR with *spry1*-specific primers +20 and −137 was used to detect *spry1* promoter sequences. In a parallel experiment protein G-Sepharose was boiled in 1× Laemmli buffer after the washes and processed for WT1 immunoblotting.

RNA Analysis by RT-PCR and Northern Blot—Total RNA (TRIzol, Invitrogen) or poly(A)$^+$ RNA (Oligotex mRNA kit, Qiagen) were fractionated on a formaldehyde-agarose gel and transferred to Hybond-N membrane (Amersham Biosciences). The mouse Multiple Tissues Northern blot was from Clontech. cDNA probes ^{32}P-labeled by random priming (23) included m*spry1* (nt 1345–1652), human *SPRY1* (nt 308–1337, XM_036349), *WT1* (9), rat, and human *Actin*. To detect m*spry1* by end-point RT-PCR, RT was performed with Superscript II reverse transcriptase (Invitrogen) using 1 μg of DNase-treated total RNAs and a m*spry1* reverse primer (nt 1993–2012). Next, 1/10 of the RT was amplified with Platinium *Taq* polymerase (Invitrogen) using a m*spry1* forward (nt 1350–1370) and reverse (nt 1633–1653) primer. RT-PCR for WT1 was performed similarly with a forward (nt 1446–1464, GenBank™ M55512) and reverse (nt 1807–1827) primer. For real time RT-PCR (31), RT was performed with a human *spry1* reverse primer (5′-GATGCCCTTGACTAAGCACATG-3′). Diluted (5 μl) RT products were amplified using a PRISM® 7700 System (Applied Biosystems) in

a volume of 25 μl containing 3 mM $MgCl_2$, PCR buffer (including SYBR green and Rox reference dye), 200 μM dNTP, 5 pmol of each primer (reverse, as for RT; forward, 5′-CCGGCAGTGCCTTTGC-3′) and 0.1 unit of AmpliTaq Gold DNA polymerase (PerkinElmer Life Sciences).

Immunoblotting—A rabbit polyclonal serum was generated against a peptide corresponding to amino acids 81–93 of mSpry1 (NP_036026) and affinity-purified (Covance, Denver, PA). The glyceraldehyde-3-phosphate dehydrogenase antibody (MAB374) was purchased from Chemicon, and the WT1 antibody (C19) used in Western blot was from Santa Cruz. Total cell lysates were analyzed by SDS-PAGE and immunoblotted as described (23).

Kidney Explant in Situ Hybridization (ISH) and Immunostaining, Whole-embryo ISH—Metanephric rudiments were dissected from E11.5 embryos into minimum Eagle's medium (Invitrogen) with 10% fetal bovine serum, 20 mM glutamine and penicillin/streptomycin and grown for 1–4 days on 1-μm polycarbonate Transwell™ filters (Costar) at 5% CO_2, 37 °C. After fixation (4% paraformaldehyde in phosphate-buffered saline overnight), all ISH were performed as described with hybridizations and washes carried out at 65 °C (32). Probes corresponding to nt 1345–1652 of m*spry1* and nt 529–799 of m*spry2* (AF176905) were synthesized as described (33) but fragmented by alkaline hydrolysis. Whole-embryo ISH was performed as described (34). Antibodies for immunofluorescence included rabbit anti-Spry1 (1/500), mouse anti-WT1 (H2, DAKO, 1/100), Cy5-conjugated goat anti-rabbit IgG, and Biodipy-conjugated anti-mouse IgG.

Morpholino Oligonucleotide Assays—E12 fetal kidney pairs were dissected and grown as described (35). Morpholino oligonucleotides antisense to *spry1* (ASSpry1, GGAGTGATCTCCAGTTCCAGCAGTC) and control oligonucleotides (Ct, invert of the antisense CTGACGACCTTGACCTCTAGTGAGG or random CCTCTTACCTCAGTTACAATTTATA) were purchased from Gene Tools (Philomath, OR) and added to the medium (20 μM) daily. Because of developmental variability within litters, right and left kidneys from the same embryo were compared with each other in the following ways: (i) medium *versus* medium plus Ct morpholino oligonucleotides (morpholinos); (ii) medium plus Ct morpholinos *versus* medium plus Spry1 morpholinos; (iii) medium *versus* medium plus Spry1 morpholinos. After 3–5 days, the explants were fixed (4% paraformaldehyde), the glomeruli were labeled with peanut agglutinin (Vector Lab (36)) and counted blindly. For immunofluorescence, explants were fixed (4 h in 4% paraformaldehyde) and permeabilized overnight at 4 °C (phosphate-buffered saline, 0.05% gelatin, 0.075% saponin). Nonspecific fluorescence was blocked by ammonium chloride (0.1 M, 2 h). The following antibodies were used: Pax2 (1:500, PRB-276P, Covance), WT1 (1:500, sc-180, Santa Cruz), synaptopodin (1:300, from Dr. P. Mundel, Albert Einstein), and Alexa 488-conjugated goat-anti-rabbit IgG (1:500, Molecular Probes). Kidneys mounted on glass slides (Vectashield, Molecular Probes) were examined using a Leica TCS-SP (UV) confocal microscope.

RESULTS

Activation of spry1 Expression by Constitutive or Induced WT1 Expression—To identify WT1 target genes, we applied RDA to mRNAs extracted from parental NIH3T3 cells and WT1A-overexpressing NIH3T3 cells (WR16 (9)). cDNAs corresponding to 34 different genes were identified, and Northern blot and RT-PCR analysis confirmed that 11 of these genes were differentially expressed[2] and not previously identified as WT1 targets. Notable among these genes was a murine homologue of *Drosophila spry* (11). *Drosophila spry*, an antagonist of tracheal branching morphogenesis, was genetically shown to inhibit Ras signaling (11, 12). Given the importance of branching morphogenesis in kidney development (37) and that WT1 inhibited growth of Ras-transformed cells (38), we next determined whether *spry1* was a transcriptional target of WT1. RT-PCR analysis (Fig. 1*A*) showed that *spry1* expression was low in NIH3T3 cells and increased in WT1-expressing cell lines (WR16, WR35, WR14).

Because constitutive expression of WT1 may have induced secondary changes in the NIH3T3 cells, we confirmed *spry1* expression in systems with inducible expression of WT1. NIH3T3 cells were infected at similar efficiencies with a bicistronic virus harboring both WT1A and green fluorescent protein or a control green fluorescent protein virus. As previously shown (Fig. 1*A*, *lane 1*), basal *spry1* expression was low in NIH3T3 cells and was unaffected by infection with a control retrovirus (Fig. 1*B*, *lane 1*). In contrast, infection with retrovirus encoding WT1 markedly increased *spry1* expression. The up-regulation occurred in parallel with the accumulation of WT1 and was observed as early as 24 h after infection (Fig. 1*B*, *lanes 2–4*).

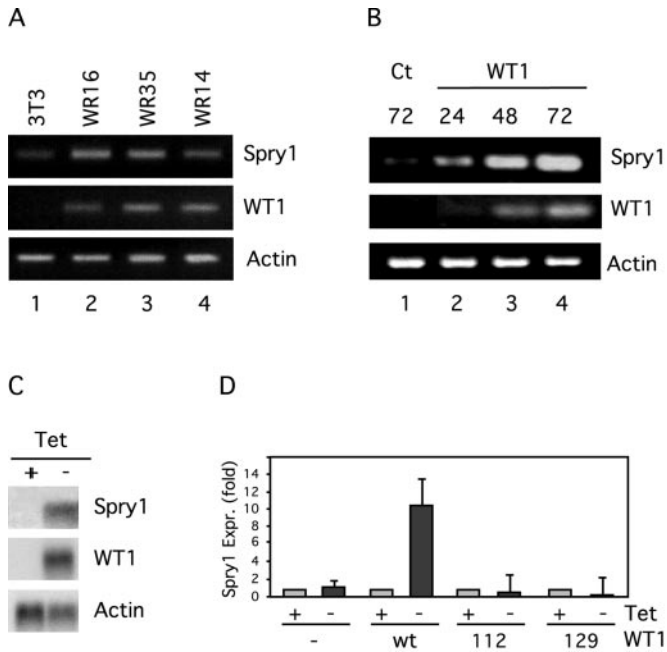

FIG. 1. **Confirmation of *spry1* as a WT1 target gene.** *A*, RT-PCR showing up-regulation of *spry1* expression in NIH3T3 cell lines constitutively expressing WT1. Actin primers were used as internal control. *B*, RT-PCR demonstrating up-regulation of *spry1* expression upon retrovirus-mediated WT1 expression. NIH3T3 cells were infected with control (*Ct*) or WT1-encoding retrovirus (*WT1*) and harvested 24, 48, or 72 h later. *C*, Northern blot (5 μg of poly(A)$^+$ RNA/lane) showing induction of *spry1* expression after induction of WT1 expression in Tet-off osteosarcoma Saos-2 cells. Actin probe was used as a loading control. *D*, quantification by real time PCR of changes in *spry1* expression (*Expr.*) 24 h after induction of wild type (*wt*) or mutant forms (F112Y, P129L) of WT1 in Tet-off Saos-2 cells.

Saos-2 cells with tetracycline-induced expression of WT1 undergo growth arrest and apoptosis (Ref. 8 and data not shown). After WT1 expression, a 2.4-kb *spry1* transcript was readily induced in these cells (Fig. 1*C*). *spry1* levels increased about 10-fold (Fig. 1*D*) as determined by quantitative real time PCR. Inducible expression of two tumor-associated WT1 missense mutants (F112Y and P129L) that yield proteins defective for transcriptional activation (27) failed to up-regulate *spry1* (Fig. 1*D*). Thus, in three different systems, endogenous *spry1* expression was activated by WT1.

WT1 Directly Activates the spry1 Promoter—To determine whether WT1 directly activates *spry1* expression, regulatory sequences for this gene were cloned and sequenced (accession number AY260058), and the start site of transcription was mapped by primer extension (data not shown). Within the proximal promoter region (1.1 kb), 8 GC-rich sites were identified (Fig. 2*A*), matching to varying degrees previously characterized WT1 binding sites: WRE (39), WTE (40), EGR1, and synthetic sites (6). This 1.1-kb segment was linked to a luciferase reporter and co-expressed in NIH3T3 cells with WT1A. WT1A activated the reporter by a factor of 8 (Fig. 2*B*), consistent with the magnitude of induction observed *in vivo* (Fig. 1*D*). In contrast, activation-defective WT1A mutant proteins (F112Y, P129L, and F154S (27)) failed to significantly activate

[2] I. Gross, B. Bassit, and J. D. Licht, manuscript in preparation.

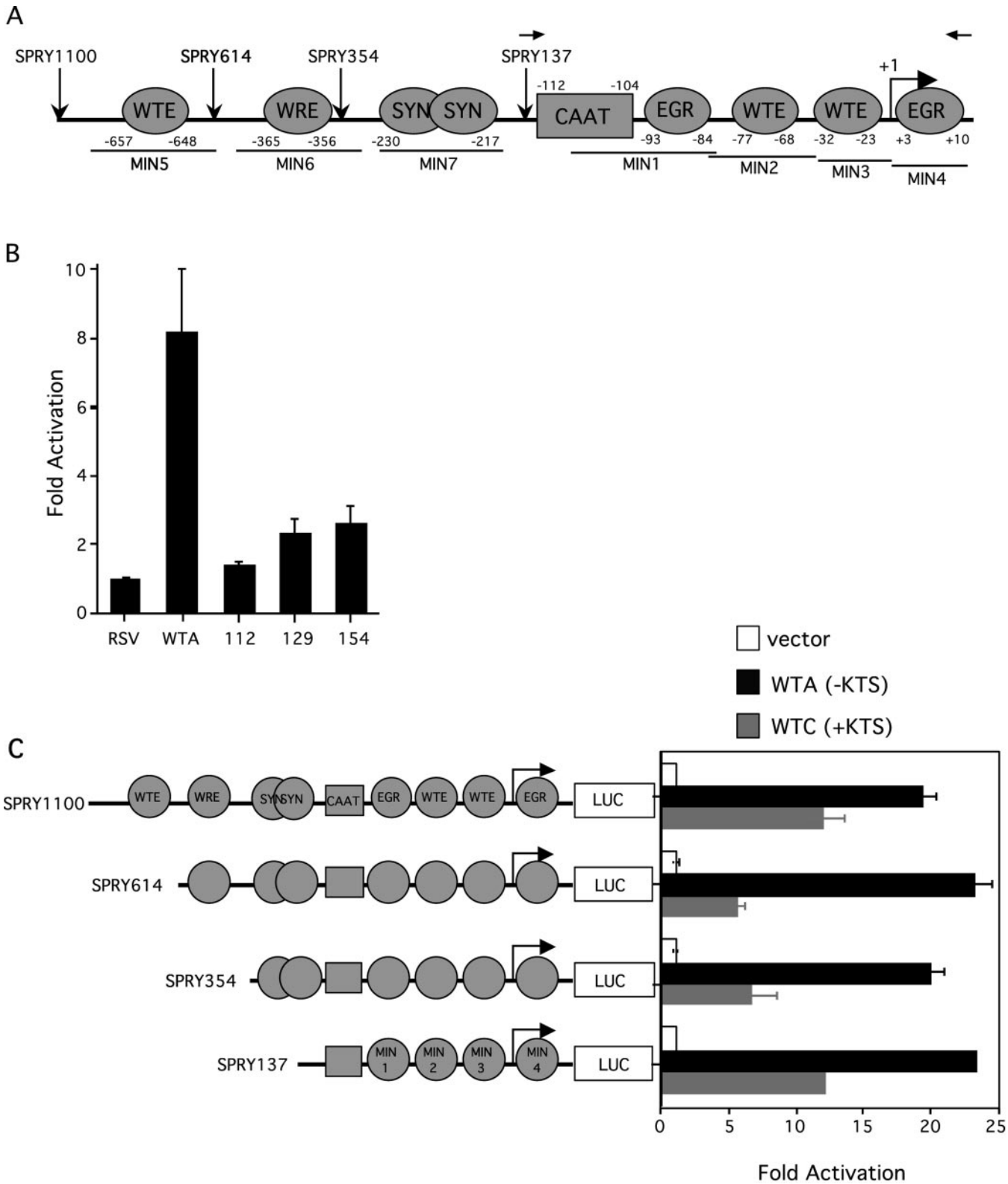

FIG. 2. **WT1 directly activates the *spry1* promoter.** *A*, diagram of *spry1* proximal promoter, indicating the location of putative WT1 binding sites. *Top arrows* mark the position of PCR primers for chromatin immunoprecipitation analysis. *B*, the full-length *spry1* reporter was transiently co-transfected into NIH3T3 cells with either a control vector (Rous sarcoma virus) or one for wild type or the indicated mutant form of WT1 (F112Y, P129L, F154S) and a *Renilla* internal control vector. Activity was measured by a dual luciferase assay. The assay was performed in triplicate (±S.D.). *C*, a series of truncations of the *spry1* promoter was tested for transactivation by WT1A and C isoforms.

the *spry1* promoter (Fig. 2*B*), although these proteins bound DNA (data not shown).

To map the WT1-responsive site, a series of truncated promoter constructs (Fig. 2*A*) was co-transfected into NIH3T3 cells with WT1. The shortest promoter fragment, SPRY137, contained four potential binding sites and was still activated by WT1 (Fig. 2*C*). The WT1C isoform (+KTS) was about 50% as active as the WT1A (−KTS) isoform.

Duplex oligonucleotide probes (MIN 1–4) spanning the GC-rich SPRY137 minimal promoter and encompassing the 4 pu-

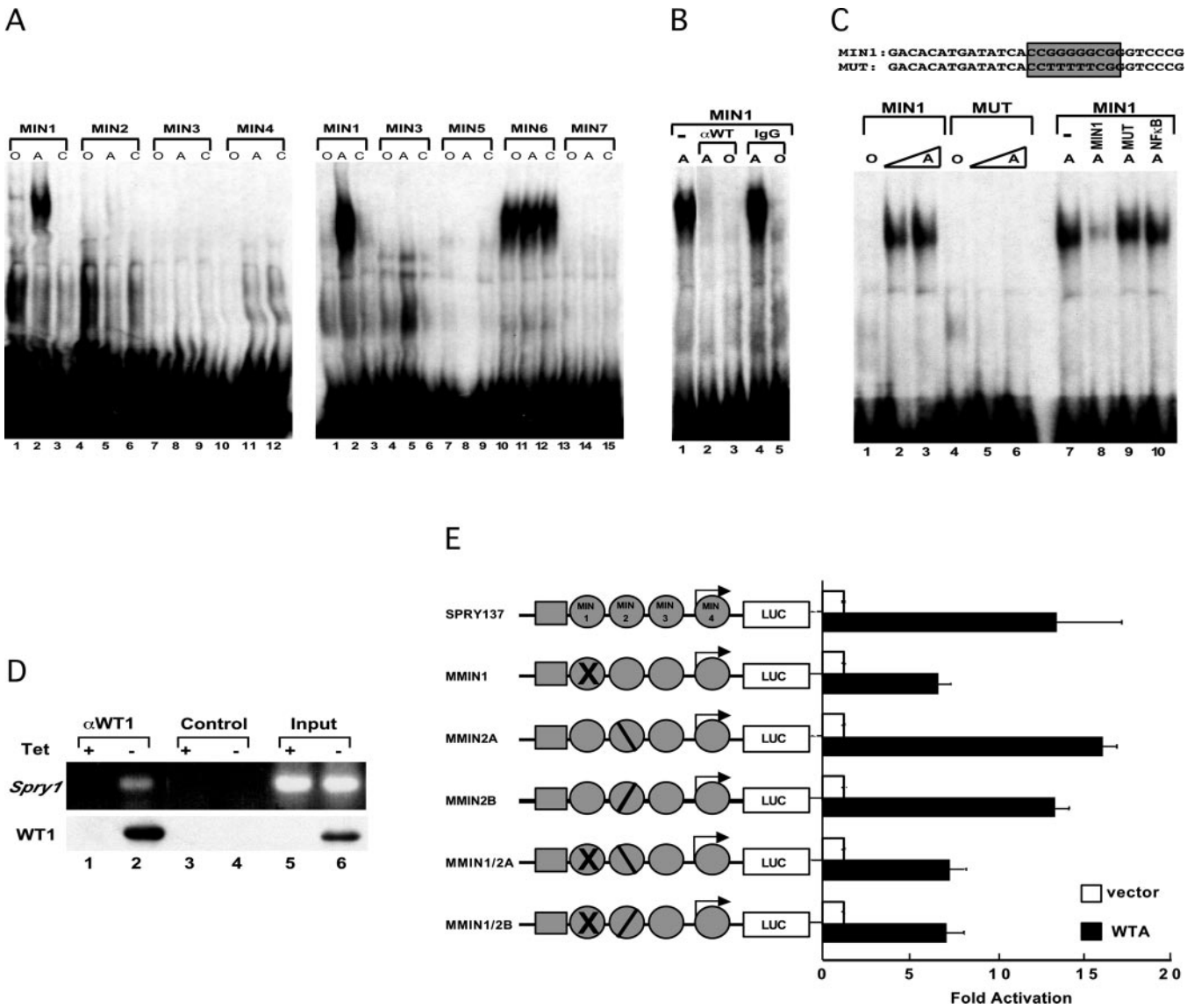

FIG. 3. **WT1 directly binds to a minimal region of the *spry1* promoter.** *A*, *panels 1* and *2*, oligonucleotide probes corresponding to all putative WT1 binding sites within the *spry1* promoter were incubated with rabbit reticulocyte lysate (*O*), *in vitro* expressed WT1A (*A*) or WT1C (*C*). *B*, WT1 antibody (*lanes 2* and *3*) or rabbit IgG (*lanes 4* and *5*) were added for supershift analysis of MIN1/WT1A complex. *C*, competition analysis was performed with a 1000× excess of homologous unlabeled MIN1 probe (*lane 8*), mutant MIN1 (*lane 9*), or an irrelevant binding site (NF-κB, *lane 10*). *D*, chromatin immunoprecipitations were performed from cells lysates cross-linked in the absence (*Tet*+) or presence (*Tet*−) of WT1A and immunoprecipitated with WT1 antibody (*lanes 1* and *2*) or no antibody control (*lanes 3* and *4*). 1% of total input chromatin demonstrates the presence of *spry1* in both sets of lysates (*lanes 5* and *6*). Western blot for WT1 in *bottom panel* shows presence of WT1 in lysates and immunoprecipitates. *E*, internal mutations were introduced into the SPRY137 promoter and tested for transactivation by WT1A.

tative WT1 binding sites and 3 additional probes (MIN 5–7) encompassing the four upstream sites were incubated with *in vitro* transcribed/translated WT1A and WT1C and subjected to a gel mobility shift assay. A strong, specific DNA-protein complex was only formed between WT1A and the MIN1 probe, corresponding to the 5′ EGR1-like site within the 137-bp promoter fragment (Fig. 3*A*, *left*, *lane 2*). On a long exposure, a weak complex was observed with the MIN2 probe (Fig. 3*A*, *left*, *lane 5*). WT1C did not bind to any of the DNA probes. Unprogrammed and programmed lysates formed a nonspecific complex with the MIN6 probe (Fig. 3*A*, *right*, *lanes 10–12*). The MIN1·WT1A complex was blocked by a WT1 antibody but not a control antibody (Fig. 3*B*, *lanes 2* and *4*). A mutant form of the EGR1 site with all 5 critical G residues mutated to T failed to bind to WT1A (Fig. 3*C*, *lanes 5* and *6*). Unlabeled MIN1 probe could compete with itself for WT1A binding (Fig. 3*C*, *lane 8*), whereas the mutant probe and an unrelated NF-κB probe could not (Fig. 3*C*, *lanes 9* and 10). Therefore, WT1A binds directly to a single EGR1 site within the minimal SPRY137 promoter. Finally, to show that WT1A bound to the *spry1* promoter *in vivo*, a chromatin immunoprecipitation was performed using NIH3T3 cells that express WT1A under tetracycline control (28). Withdrawal of tetracycline induced the expression of WT1A (Fig. 3*D*, *lanes 5 versus 6*). Only in the presence of WT1A was the *spry1* promoter precipitated by a WT1 antibody (Fig. 3*D*, *lanes 1 versus 2*) along with the WT1 protein.

Mutation of the MIN1 site in the context of the SPRY137 luciferase reporter reduced WT1-mediated transactivation by 50% (Fig. 3*E*). Two different mutations of MIN2, which weakly bound WT1A *in vitro*, had no effect on WT1 transactivation either alone or in combination with the MIN1 mutation (Fig. 3*E*). Taken together the data indicate that WT1 activates transcription through direct binding to an EGR1 site within the *spry1* promoter. The residual transactivation in the presence of a mutated MIN1 site might be due to the adjacent CAAT box sequence, which we previously showed to promote WT1 trans-

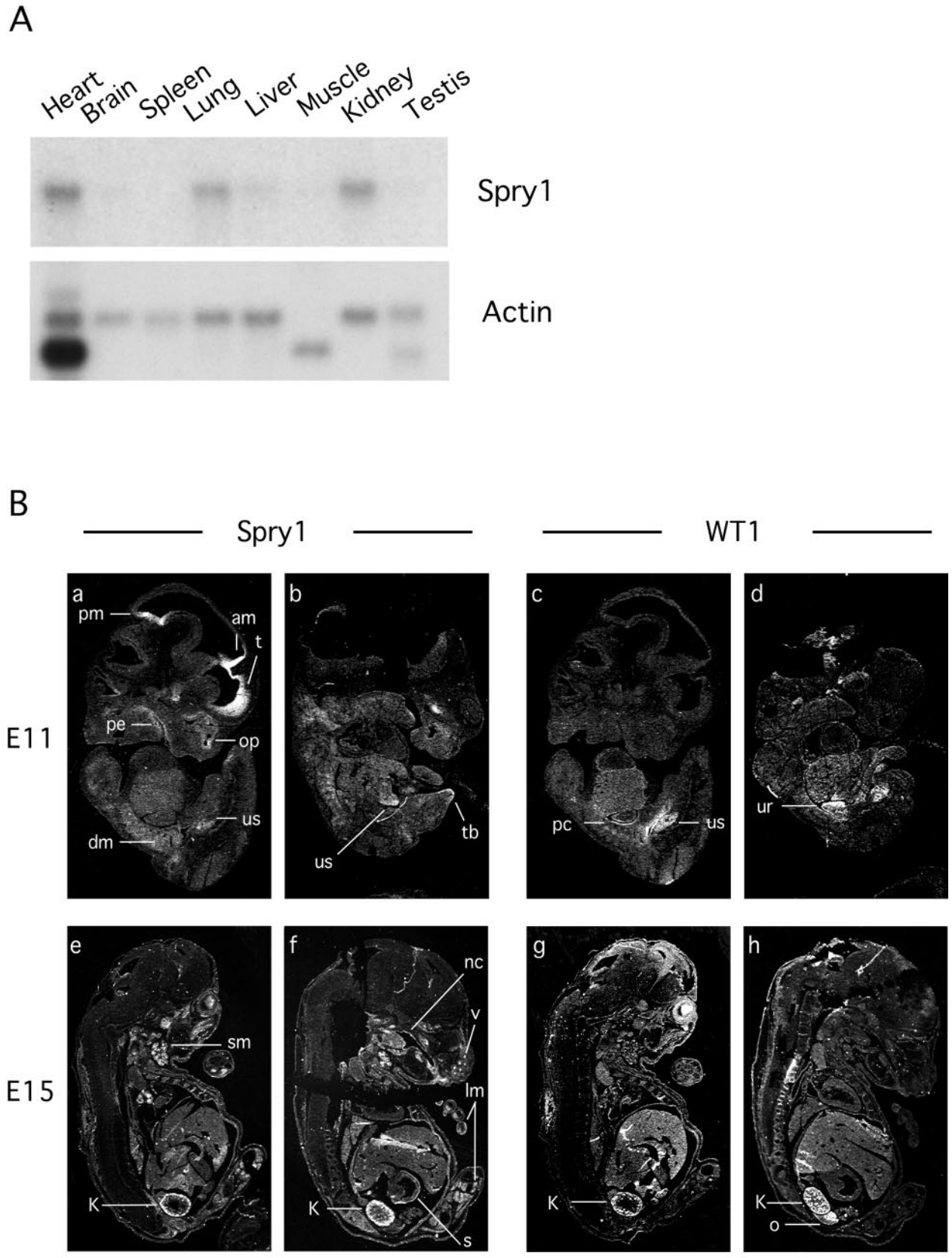

FIG. 4. **Expression of *spry1* in adult mouse tissues and in the murine embryo.** *A*, *spry1* is detected by Northern blot in several adult mouse tissues, including the kidney. The filter was re-probed with actin to verify RNA integrity. *B*, ISH with mouse whole embryo sagittal sections using a ^{35}S-labeled *spry1* antisense riboprobe (*a*, *b*, *e*, and *f*) or a *wt1* antisense riboprobe (*c*, *d*, *g*, and *h*). *spry1* expression is detected in the urogenital sinus and the kidney at E11 and E15 as well as several other developing organs/tissues. *wt1* expression is mostly restricted to the maturing urogenital tract. *am*, anterior wall of midbrain; *dm*, dermomyotome; *k*, kidney; *lm*, limb muscle; *o*, ovary; *nc*, nasal cavity; *op*, olfactory pit; *pc*, peritoneal cavity; *pe*, pharingeal epithelium; *pm*, posterior wall of midbrain; *s*, stomach; *sm*, submandibular gland; *t*, roof of telencephalon; *tb*, tail bud; *ur*, urogenital ridge; *us*, urogenital sinus; *v*, vibrissae primordium.

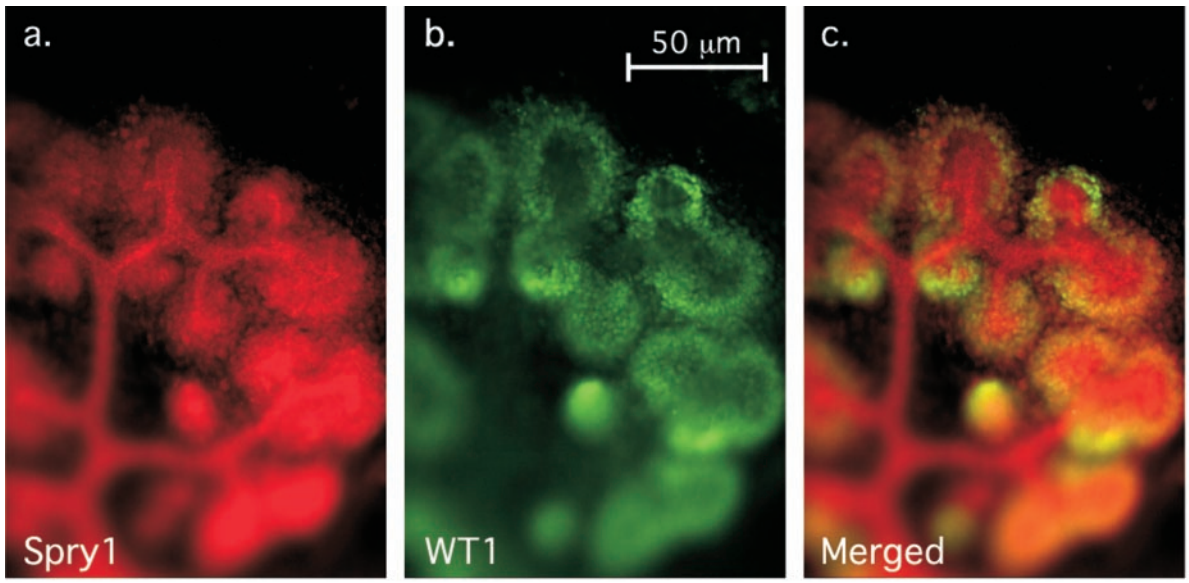

FIG. 5. **Co-expression of Spry1 and WT1 in the developing kidney.** Four-day mouse kidney explants were simultaneously incubated with a polyclonal rabbit serum recognizing Spry1 (*a*) and a monoclonal mouse antibody to WT1 (*b*). Spry1 was visualized with the Cy3-conjugated antibodies against rabbit IgG, and WT1 was detected using Biodipy-conjugated antibodies against mouse IgG. Image *c* represents the merged signals of the preceding *two panels* (*ab*). Spry1 protein is detected in both the condensing mesenchyme and the ureteric tree, whereas WT1 is only present in the differentiating mesenchyme. Because WT1 is a nuclear protein and Spry1 a cytoplasmic protein, the dual signal does not generally appear yellow.

activation (28). This explanation is consistent with the ability of WT1C to transactivate in the absence of DNA binding.

Expression of spry1 during Kidney Development—To determine the relationship between *spry1* and *wt1*, the expression pattern of *spry1* was examined. In adult mouse tissues, *spry1* transcripts were detected by Northern blot in heart, lung, and most importantly, kidney (Fig. 4*A*). Next, we compared the expression of *wt1* and *spry1* during embryonic development. ISH of whole-embryo sections detected *spry1* transcripts in several developing organs, including the urogenital sinus, the tail bud, and parts of the midbrain (Fig. 4*B*, *a–b*). Robust labeling of the developing kidney was observed at E15 (Fig. 4*B*, *e–f*). *wt1* exhibited highly tissue-specific expression mostly restricted to the maturing urogenital tract (Fig. 4*B*, *c–d* and *g–h* and Ref. 41 and 42). Prominent *wt1* expression at E11 preceded the high level *spry1* expression at E15, consistent with the notion that WT1 is an upstream regulator of *spry1*.

To further correlate Spry1 and WT1 expression, murine kidney rudiments from E11.5 embryos were cultured for 4 days and analyzed by immunofluorescence. Spry1 was detected in both the condensing mesenchyme and the ureteric tree (Fig. 5*a*). Moreover, double-labeling experiments using a monoclonal anti-WT1 antibody demonstrated concordant expression of WT1 and Spry1 proteins in the condensing metanephric mesenchyme (Fig. 5, *b* and *c*). Because WT1 is a nuclear protein and Spry 1 is a cytoplasmic protein (19), the staining did not exactly overlay. Nevertheless, these data suggest that *spry1* is involved in the development of the embryonic kidney and are consistent with the notion that WT1 can control *spry1* expression.

To map the expression of *spry1* during kidney development, explants from E11.5 embryos were cultured for 1–4 days and subjected to ISH. *spry1* exhibited a dynamic pattern during renal development (Fig. 6. *A–E*). As the ureteric bud invaded the metanephric blastema, strong *spry1* expression was observed in the metanephric mesenchyme condensing around the tips of the ureteric buds (Fig. 6*A*, condensing mesenchyme (*cm*) and *arrow*). The ureteric tree showed weaker expression of *spry1* mRNA (Fig. 6*B*, *arrow*). As the explant matured, *spry1* was also expressed in the comma- and S-shaped bodies (Fig. 6*C* and Fig. 6*E*, comma bodies (*cb*)) as well as in the ureteric tree (Fig. 6, *C* and *D*, *arrows*). *wt1*, as reported (41, 42), was expressed in the differentiating blastema but not in the ureteric tree (Fig. 6*F*). Therefore, *wt1* and *spry1* expression was coincident in both the uninduced and the condensing mesenchyme. ISH performed on paraffin sections of embryonic kidneys gave similar results (data not shown).

Murine *spry1* belongs to a family of genes often co-expressed during embryogenesis (13, 14, 26, 43). As a control for the specificity of *spry1* as a WT1 target gene in the kidney, *spry2* expression was also examined (Fig. 6, *G* and *H*). *spry2* was first expressed in the ureteric bud as it invaded the metanephric mesenchyme. It was not restricted to the ureteric epithelium but extended into the adjacent mesenchyme (Fig. 6*G*, *asterisks*). In more mature explants, *spry2* decreased in the ureteric epithelium and was expressed in renal stromal cells surrounding the mesenchyme undergoing epithelial transition (Fig. 6*H*, ′′). In contrast to *spry1*, *spry2* was neither expressed in the condensing metanephric blastema nor in the comma- and S-shaped bodies. Thus, expression of *spry1* suggests a specific role for this particular gene during metanephric development.

Disruption of Spry1 Expression in Embryonic Kidney Explants—To gain insight into the possible role of *spry1* during kidney development, we used antisense morpholinos, reported to be more specific than traditional oligonucleotides (44), to examine the consequences of disruption of *spry1* expression in the developing metanephric kidney. Paired murine kidney rudiments were isolated from E12 embryos and grown in culture for 3 days in the absence or presence of morpholinos before fixation and staining. Explants grown in the presence of *spry1* antisense morpholinos were normal in size but exhibited a 50% reduction in the number of developing and mature glomeruli (visualized by peanut lectin staining of visceral podocytes (45); Fig. 7, *A*, *a–b*, and *B*). This effect was specific, as explants treated with control morpholinos (invert of the antisense or random) developed normally. The number of ureteric branches and tips (visualized by Dolichos bifloris lectin staining (45)) that formed in the kidney explants treated with *spry1* morpholinos (and exhibiting less glomeruli) was not significantly different from control explants (data not shown). However, histochemical sections revealed that ureteric trees from antisense-

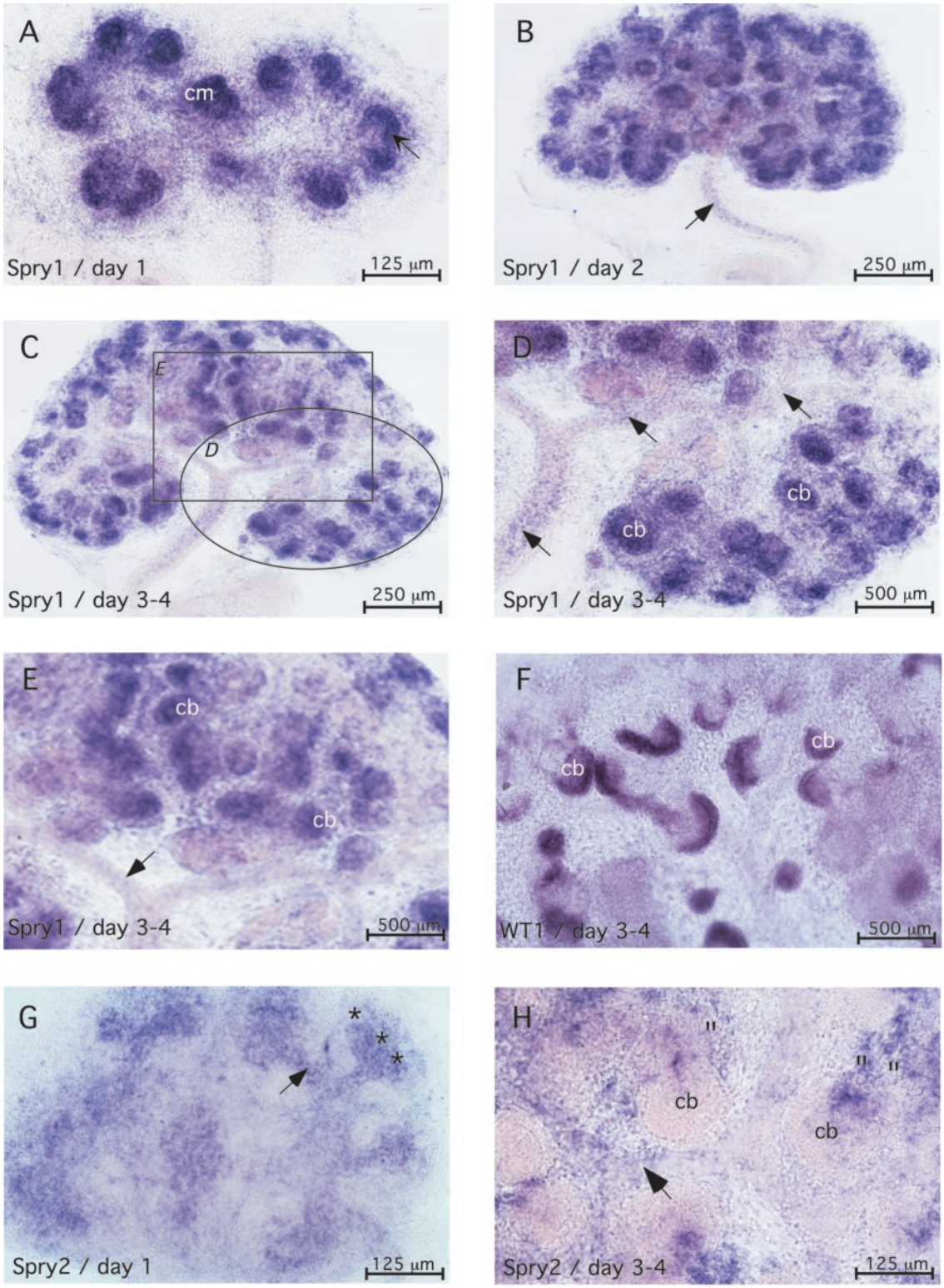

FIG. 6. **Expression of *spry1* and *spry2* in murine kidney explants.** Metanephric kidney rudiments were isolated from E11.5 embryos and cultured for 1–4 days before whole-mount ISH with antisense riboprobes. *A*, 1-day explant showing weak *spry1* expression in the ureteric canal and intense expression in the condensing mesenchyme (*cm*) immediately surrounding the ends of the tips of the ureteric tree. The *arrow* points to a branch point near the tip of the invading ureteric bud. *B*, 2-day explant showing *spry1* expression in the condensing mesenchyme, the comma-shaped bodies, and the ureteric tree (*arrow*). *C*, 3–4-day explant with *spry1* expression still highest in the condensing mesenchyme. *D*, magnification of the circled area in *C* showing weak *spry1* expression in the ureteric tree (*arrows*). *E*, magnification of the squared area in *C* showing *spry1* expression in the comma (*cb*)- and S-shaped bodies as the MET occurs. *F*, 3–4-day explant showing *wt1* expression in the condensing mesenchyme, the comma (*cb*)- and S-shaped bodies. *G*, 1-day explant showing *spry2* expression along the ureteric tree (*arrow*) as it invaded the metanephric mesenchyme. *spry2* expression extended in the adjacent mesenchyme (*). *H*, 3–4-day explant with weaker expression of *spry2* in the ureteric tree (*arrows*) and in between the mesenchyme that had undergone MET (''; no *spry2* expression was detected in the comma (*cb*)- or S-shaped bodies.

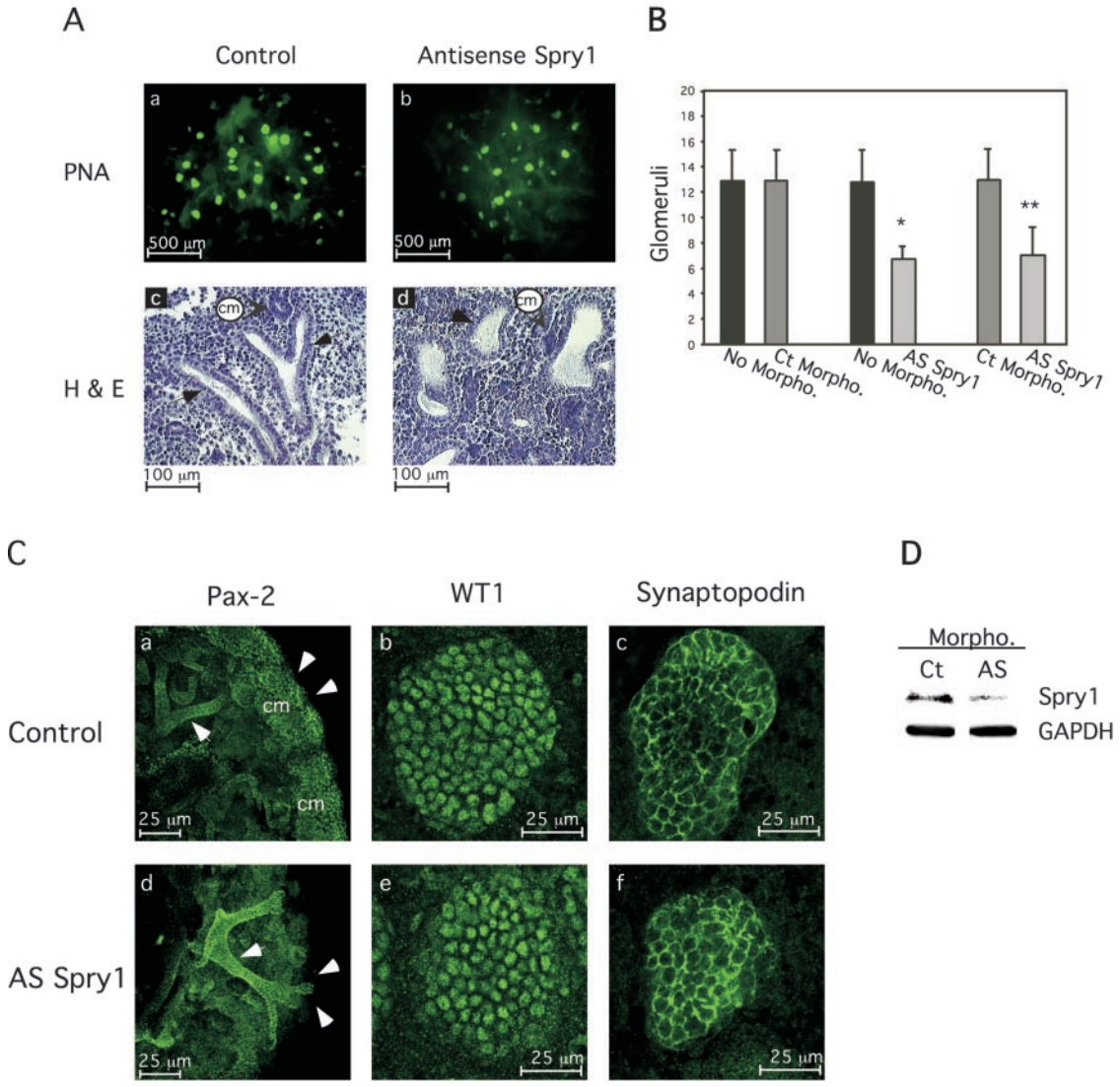

FIG. 7. **Disruption of Spry1 expression by antisense morpholinos affects nephrogenesis in embryonic kidney explants.** *A*, paired E12 mouse kidney explants grown for 3 days in medium with 20 μM of *spry1* antisense or control morpholinos. To visualize glomeruli, whole-mount immunofluorescence with peanut agglutinin (*PNA*) was done (*a* and *b*). Sections were stained with hematoxylin/eosin to see ureteric tree morphology upon treatment with morpholinos. *c* and *d*: *cm*, condensing mesenchyme; *arrow*, ureteric tree. Similar results were obtained in six other experiments. *B*, the number of glomeruli formed was counted for each pair of kidneys (6 or 7 pairs for each condition, see "Materials and Methods"), and the average ± S.E. is presented. *Ct morpho.*, control morpholino (invert of the antisense); *AS morpho*, *spry1* antisense morpholino. *, $p < 0.003$, and **, $p < 0.001$, by χ^2. *C*, whole mount confocal immunofluorescence for Pax2 (*a* and *d*, magnification 10×), WT1 (*b* and *e*, magnification 40×) and synaptopodin (*c* and *f*, magnification 40×) showing reduced condensation of the metanephric mesenchyme (*arrowheads*) in the explants treated with *spry1* morpholinos but normal glomeruli. *D*, Western blot showing decreased Spry1 expression in renal IMCD-3 cells following *spry1* antisense (*AS*) treatment. A glyceraldehyde-3-phosphate dehydrogenase antibody was used to assure equal protein loading.

treated kidneys tended to be less elongated between branch points and had wider, cystic, tubular lumens (Fig. 7*A*, *c–d*).

The explants were further characterized using different markers of renal development. Pax2, a marker of early metanephric development (46), was detected in the induced mesenchyme condensing around the ureteric bud of control explants (Fig. 7*C*, *a*). In contrast, expression of Pax2 was strikingly reduced in the antisense-treated explants (Fig. 7*C*, d*)*, indicating a lack of condensation. Additional immunofluorescence with antibodies against markers of the mature glomerulus, such as synaptopodin (47) and WT1 (48), confirmed that the glomeruli formed in the antisense-treated explants were morphologically normal (Fig. 7*C*, *b*, *e* and *c*, *f*). Thus, the reduced number of glomeruli observed in the antisense-treated explants was caused by a defect in the earliest phase of epithelialization.

Given that *spry1* morpholinos reduced the number of nascent glomeruli and that these structures normally express Spry1 during kidney development, we checked the efficiency of the morpholinos in cultured renal cells to avoid an inherent bias of using treated kidneys. IMCD-3 cells (29) treated with *spry1* morpholinos expressed less Spry1 compared with cells treated with controls (Fig. 7*D*). Taken together, these data suggest that appropriate Spry1 expression is important for the development of both the metanephric blastema and the ureteric tree.

DISCUSSION

In the present study we have used RDA to identify *spry1* as a target gene of WT1, a transcription factor involved in renal development and tumorigenesis. *spry1* belongs to a newly identified family of receptor tyrosine kinase modulators, and our study is the first one to identify one of their transcriptional regulators. Endogenous *spry1* expression was activated upon constitutive or acute expression of WT1 in NIH3T3 fibroblasts. Wild-type, but not transactivation-deficient forms of WT1, induced *spry1* expression in Saos-2 cells. WT1 directly bound to the *spry1* promoter both *in vitro* and *in vivo* and transactivated

its expression in reporter assays through a GC-rich EGR1 binding site. Overlapping expression of *wt1* and *spry1* in condensing metanephric blastemal cells and developing glomeruli suggests that *spry1* represents a physiologically relevant target gene of WT1. However, the regulation of *spry1* in the kidney may be complex as expression in the ureteric tree must occur independent of WT1 expression, which is absent in this structure. Therefore, transcription factors present in both the ureteric tree and the condensing mesenchyme, such as Pax2, might also regulate *spry1* expression (49).

WT1 as a Transcriptional Activator—The identity of WT1 targets and the transcriptional function of WT1 have been controversial (2). WT1 was previously thought to inhibit cell proliferation by repression of growth-promoting genes. However, a survey using several cellular models failed to confirm regulation of 16 genes proposed to be repressed by WT1 (50). This information suggested that the initial characterization of WT1 as a transcriptional repressor needed to be re-evaluated. Now data from our group and others indicate that WT1 functions by activating growth suppressor genes such as *spry1*, *p21*, or *E-cadherin* (27, 28, 51) and inducing genes required for the differentiation of the kidney such as *podocalyxin* (52). Eight of 11 genes identified in our RDA screen were activated by WT1 and using microarray analysis, Lee *et al.* (39) only found genes activated by WT1. Previously, our group demonstrated that three Wilms tumor-derived point mutations that abrogate the growth inhibition by WT1 were competent for transcriptional repression but defective for transcriptional activation of reporter genes (27). These same point mutants failed to upregulate the endogenous *spry1* gene. Thus, the transcriptional activation properties of WT1, once controversial, appear now to be critical for its biological role.

Analysis of the *spry1* promoter revealed eight potential WT1 binding sites; of these, only the 5′EGR1 site was a complete match to known WT1 sites, and only this site strongly bound WT1. Consistent with prior reports, WT1 could also transactivate without direct DNA binding (28). For example, the *E-cadherin* promoter, like that of *spry1*, contains a CAAT box immediately upstream of the EGR1 site (28). This CAAT box supported minimal WT1 transactivation in the presence of a mutation in the EGR1 site even though WT1 did not bind directly to this element. In the *amphiregulin* promoter, the CRE (cAMP-response element) adjacent to the WT1 binding site was responsive to WT1 while not being directly bound by WT1 (39). This was possibly due to protein-protein interactions between WT1 and CBP (CREB-binding protein), a co-activator of CRE binding factors. Finally, WT1 associated and synergized with the steroidogenic factor 1 to activate müllerian inhibiting substance expression (53). Steroidogenic factor 1, but not WT1, bound to the müllerian inhibiting substance promoter. The identification of additional WT1 co-factors, potentially those that bind to the CAAT box, will help explain the full range of WT1 activity.

Possible Roles for Spry1 during Kidney Development—Induction of the metanephric blastema by the invading ureteric bud is a key step in kidney development. The ureteric bud grows out from the wolffian duct and into the metanephric mesenchyme, where it branches and induces nephron formation (54). Mesenchymal cells of the blastema condense around the ureteric bud, undergo a MET, and form the nephric epithelium. This tightly controlled process involves changes in cell survival, proliferation, and differentiation. WT1 is expressed in the induced blastemal cells and plays a key role in this process. *WT1* null mice lack kidneys (5) and mice that do not express the −KTS isoforms of WT1 (WT1A and WT1B) demonstrate a decrease in the nephrogenic zone and a reduction of the number of glomeruli (55). Moreover, the MET is disrupted in Wilms tumors with a direct correlation between the level of WT1 expression and the degree of epithelial differentiation (56).

As expected of a potential WT1 effector, Spry1 was shown to inhibit proliferation of mesenchymal cells (23). Like WT1, Spry1 is expressed in the condensing mesenchyme and may relay some of the activity of WT1 during nephrogenesis. For instance, treatment of kidney explants with s*pry1* morpholinos led to fewer mature glomeruli and a defect in Pax2 expression, suggesting a failure of induction of the metanephric mesenchyme adjacent to the ureteric bud. Strikingly, mice deficient for the −KTS isoforms of WT1 showed a similar lack of mesenchyme condensation (55). WT1 expression is also required for the proper formation and maintenance of the glomerulus (55, 57). However, microscopic and immunofluorescence analysis of those glomeruli that did form in the presence of *spry1* morpholinos did not reveal any striking difference in morphology. This could be due to an incomplete suppression of Spry1 expression by the morpholinos. Alternatively, this might indicate that Spry1 modulates the threshold of growth factor signaling that allows epithelial differentiation and glomerulus formation but is dispensable for the maintenance of the differentiated phenotype. Further analysis will be required to understand the exact role of Spry1 in nephrogenesis, but the results presented here suggest an important role for *spry1* in the early stages of the MET in the metanephric blastema and support its identification as a WT1 target gene.

Spry1 also plays a role in the development of the ureteric tree. Given that WT1 is not expressed in this structure, *spry1* must be under the control of other transcription factors in this region. Treatment of kidneys with *spry1* morpholinos was associated with an altered, cystic morphology of the ureteric tree. Because Spry proteins can inhibit proliferation or migration of epithelial cells, disruption of Spry1 expression could result in deregulated growth factor signaling and expansion of the ureteric epithelial lining. In support of this notion, epidermal growth factor treatment of kidney explants (58) or excessive glial-derived nerve growth factor signaling in mice[3] leads to the formation of similar abnormal cystic tubules. Lack of *spry* expression enhanced branching morphogenesis of the tracheal system in the fly (11). In contrast, we did not detect a change in the number of ureteric tree branches in antisense-treated murine explants. This may be due to incomplete suppression of Spry1 or partial rescue by Spry2 in the ureteric tree.

Initial studies did not reveal functional differences between the different Spry members, so it was postulated that the Spry proteins may play redundant roles (14). However, this does not appear to be true in the kidney. *spry2* was expressed in a distinctly different pattern from *spry1*, and WT1 could not induce the expression of *spry2* or *spry4* (data not shown). Hence, the expression pattern of *spry1* in the kidney and its relationship with WT1 are specific.

In conclusion, our results suggest that *spry1* is a *bona fide* WT1 target gene. Spry1, by regulating receptor tyrosine kinase-dependent Ras signaling, may contribute to several stages of kidney development. Future studies of gene-targeted animals and organ culture models will further clarify the role of the *spry* genes during mammalian kidney development.

Acknowledgments—We thank Drs. C. R. Burrow and C. Gaiddon for advice and discussion, Dr. D. Haber for the WT1 Tet-off Saos-2 cells, and Dr. P. Mundel for the synaptopodin antibody. We acknowledge B. Bassit for technical assistance and Dr. A. Basson for help subcloning the *spry1* promoter.

[3] F. Costantini, personal communication.

REFERENCES

1. Kuure, S., Vuolteenaho, R., and Vainio, S. (2000) *Mech. Dev.* **92,** 31–45
2. Reddy, J. C., and Licht, J. D. (1996) *Biochim. Biophys. Acta* **1287,** 1–28
3. Little, M., Holmes, G., and Walsh, P. (1999) *Bioessays* **21,** 191–202
4. Lee, S. B., and Haber, D. A. (2001) *Exp. Cell Res.* **264,** 74–99
5. Kreidberg, J. A., Sariola, H., Loring, J. M., Maeda, M., Pelletier, J., Housman, D., and Jaenisch, R. (1993) *Cell* **74,** 679–691
6. Rauscher, F. J., III, Morris, J. F., Tournay, O. E., Cook, D. M., and Curran, T. (1990) *Science* **250,** 1259–1262
7. Wang, Z. Y., Qiu, Q. Q., Enger, K. T., and Deuel, T. F. (1993) *Proc. Natl. Acad. Sci. U. S. A.* **90,** 8896–8900
8. Englert, C., Hou, X., Maheswaran, S., Bennett, P., Ngwu, C., Re, G. G., Garvin, A. J., Rosner, M. R., and Haber, D. A. (1995) *EMBO J.* **14,** 4662–4675
9. Hosono, S., Luo, X., Hyink, D. P., Schnapp, L. M., Wilson, P. D., Burrow, C. R., Reddy, J. C., Atweh, G. F., and Licht, J. D. (1999) *Oncogene* **18,** 417–427
10. Hubank, M., and Schatz, D. G. (1994) *Nucleic Acids Res.* **22,** 5640–5648
11. Hacohen, N., Kramer, S., Sutherland, D., Hiromi, Y., and Krasnow, M. A. (1998) *Cell* **92,** 253–263
12. Casci, T., Vinos, J., and Freeman, M. (1999) *Cell* **96,** 655–665
13. Chambers, D., and Mason, I. (2000) *Mech. Dev.* **91,** 361–364
14. Minowada, G., Jarvis, L. A., Chi, C. L., Neubuser, A., Sun, X., Hacohen, N., Krasnow, M. A., and Martin, G. R. (1999) *Development* **126,** 4465–4475
15. Nutt, S. L., Dingwell, K. S., Holt, C. E., and Amaya, E. (2001) *Genes Dev.* **15,** 1152–1166
16. de Maximy, A. A., Nakatake, Y., Moncada, S., Itoh, N., Thiery, J. P., and Bellusci, S. (1999) *Mech. Dev.* **81,** 213–216
17. Furthauer, M., Reifers, F., Brand, M., Thisse, B., and Thisse, C. (2001) *Development* **128,** 2175–2186
18. Tefft, D., Lee, M., Smith, S., Crowe, D. L., Bellusci, S., and Warburton, D. (2002) *Am. J. Physiol. Lung Cell. Mol. Physiol.* **283,** 700–706
19. Impagnatiello, M. A., Weitzer, S., Gannon, G., Compagni, A., Cotten, M., and Christofori, G. (2001) *J. Cell Biol.* **152,** 1087–1098
20. Sasaki, A., Taketomi, T., Wakioka, T., Kato, R., and Yoshimura, A. (2001) *J. Biol. Chem.* **276,** 36804–36808
21. Egan, J. E., Hall, A. B., Yatsula, B. A., and Bar-Sagi, D. (2002) *Proc. Natl. Acad. Sci. U. S. A.* **99,** 6041–6046
22. Wong, E. S., Fong, C. W., Lim, J., Yusoff, P., Low, B. C., Langdon, W. Y., and Guy, G. R. (2002) *EMBO J.* **21,** 4796–4808
23. Gross, I., Bassit, B., Benezra, M., and Licht, J. D. (2001) *J. Biol. Chem.* **276,** 46460–46468
24. Yusoff, P., Lao, D. H., Ong, S. H., Wong, E. S., Lim, J., Lo, T. L., Leong, H. F., Fong, C. W., and Guy, G. R. (2002) *J. Biol. Chem.* **277,** 3195–3201
25. Tefft, J. D., Lee, M., Smith, S., Leinwand, M., Zhao, J., Bringas, P., Jr., Crowe, D. L., and Warburton, D. (1999) *Curr. Biol.* **9,** 219–222
26. Mailleux, A. A., Tefft, D., Ndiaye, D., Itoh, N., Thiery, J. P., Warburton, D., and Bellusci, S. (2001) *Mech. Dev.* **102,** 81–94
27. English, M. A., and Licht, J. D. (1999) *J. Biol. Chem.* **274,** 13258–13263
28. Hosono, S., Gross, I., English, M. A., Hajra, K. M., Fearon, E. R., and Licht, J. D. (2000) *J. Biol. Chem.* **275,** 10943–10953
29. Rauchman, M. I., Nigam, S. K., Delpire, E., and Gullans, S. R. (1993) *Am. J. Physiol.* **265,** F416–F424
30. Relaix, F., Wei, X. J., Wu, X., and Sassoon, D. A. (1998) *Nat. Genet.* **18,** 287–291
31. Gibson, U. E., Heid, C. A., and Williams, P. M. (1996) *Genome Res.* **6,** 995–1001
32. Kolle, G., Georgas, K., Holmes, G. P., Little, M. H., and Yamada, T. (2000) *Mech. Dev.* **90,** 181–193
33. Holmes, G. P., Negus, K., Burridge, L., Raman, S., Algar, E., Yamada, T., and Little, M. H. (1998) *Mech. Dev.* **79,** 57–72
34. Sassoon, D., and Rosenthal, N. (1993) *Methods Enzymol.* **225,** 384–404
35. Avner, E. D., Sweeney, W. E., Jr., Piesco, N. P., and Ellis, D. (1985) *In Vitro Cell. Dev. Biol.* **21,** 297–304
36. Mendelsohn, C., Batourina, E., Fung, S., Gilbert, T., and Dodd, J. (1999) *Development* **126,** 1139–1148
37. al-Awqati, Q., and Goldberg, M. R. (1998) *Kidney Int.* **54,** 1832–1842
38. Luo, X. N., Reddy, J. C., Yeyati, P. L., Idris, A. H., Hosono, S., Haber, D. A., Licht, J. D., and Atweh, G. F. (1995) *Oncogene* **11,** 743–750
39. Lee, S. B., Huang, K., Palmer, R., Truong, V. B., Herzlinger, D., Kolquist, K. A., Wong, J., Paulding, C., Yoon, S. K., Gerald, W., Oliner, J. D., and Haber, D. A. (1999) *Cell* **98,** 663–673
40. Nakagama, H., Heinrich, G., Pelletier, J., and Housman, D. E. (1995) *Mol. Cell. Biol.* **15,** 1489–1498
41. Pritchard-Jones, K., Fleming, S., Davidson, D., Bickmore, W., Porteous, D., Gosden, C., Bard, J., Buckler, A., Pelletier, J., Housman, D., van Heyningen, V., and Hastie, N. (1990) *Nature* **346,** 194-197
42. Armstrong, J. F., Pritchard-Jones, K., Bickmore, W. A., Hastie, N. D., and Bard, J. B. (1993) *Mech. Dev.* **40,** 85–97
43. Davidson, B. P., Cheng, L., Kinder, S. J., and Tam, P. P. (2000) *Dev. Biol.* **221,** 41–52
44. Summerton, J., and Weller, D. (1997) *Antisense Nucleic Acid Drug Dev.* **7,** 187–195
45. Laitinen, L., Virtanen, I., and Saxen, L. (1987) *J. Histochem. Cytochem.* **35,** 55–65
46. Rothenpieler, U. W., and Dressler, G. R. (1993) *Development* **119,** 711–720
47. Mundel, P., Reiser, J., Zuniga Mejia Borja, A., Pavenstadt, H., Davidson, G. R., Kriz, W., and Zeller, R. (1997) *Exp. Cell Res.* **236,** 248–258
48. Mundlos, S., Pelletier, J., Darveau, A., Bachmann, M., Winterpacht, A., and Zabel, B. (1993) *Development* **119,** 1329–1341
49. Dressler, G. R., Deutsch, U., Chowdhury, K., Nornes, H. O., and Gruss, P. (1990) *Development* **109,** 787–795
50. Thate, C., Englert, C., and Gessler, M. (1998) *Oncogene* **17,** 1287–1294
51. Englert, C., Maheswaran, S., Garvin, A. J., Kreidberg, J., and Haber, D. A. (1997) *Cancer Res.* **57,** 1429–1434
52. Palmer, R. E., Kotsianti, A., Cadman, B., Boyd, T., Gerald, W., and Haber, D. A. (2001) *Curr. Biol.* **11,** 1805–1809
53. Nachtigal, M. W., Hirokawa, Y., Enyeart-VanHouten, D. L., Flanagan, J. N., Hammer, G. D., and Ingraham, H. A. (1998) *Cell* **93,** 445–454
54. Schedl, A., and Hastie, N. D. (2000) *Curr. Opin. Genet. Dev.* **10,** 543–549
55. Hammes, A., Guo, J. K., Lutsch, G., Leheste, J. R., Landrock, D., Ziegler, U., Gubler, M. C., and Schedl, A. (2001) *Cell* **106,** 319–329
56. Miwa, H., Tomlinson, G. E., Timmons, C. F., Huff, V., Cohn, S. L., Strong, L. C., and Saunders, G. F. (1992) *J. Natl. Cancer Inst.* **84,** 181–187
57. Guo, J. K., Menke, A. L., Gubler, M. C., Clarke, A. R., Harrison, D., Hammes, A., Hastie, N. D., and Schedl, A. (2002) *Hum. Mol. Genet.* **11,** 651–659
58. Avner, E. D., and Sweeney, W. E., Jr. (1990) *Pediatr. Nephrol.* **4,** 372–377

The Receptor Tyrosine Kinase Regulator Sprouty1 Is a Target of the Tumor Suppressor WT1 and Important for Kidney Development

Isabelle Gross, Debra J. Morrison, Deborah P. Hyink, Kylie Georgas, Milton A. English, Mathias Mericskay, Seiyu Hosono, David Sassoon, Patricia D. Wilson, Melissa Little and Jonathan D. Licht

J. Biol. Chem. 2003, 278:41420-41430.
doi: 10.1074/jbc.M306425200 originally published online July 25, 2003
